ON THE FUNCTIONING OF A HELICOPTER-BORNE HF LOOP ANTENNA

Duncan C. Baker

Department of Electronics and Computer Engineering,
University of Pretoria, Pretoria, 0002, South Africa.

ABSTRACT: *Numerical techniques allow engineers to evaluate the performance of antennas on complex structures. These techniques can provide valuable physical insights into the overall functional performance of such antennas. This short paper reports on the use of NEC2 to investigate the radiation characteristics of a loop antenna mounted below the tailboom of a helicopter in the frequency band 2-15 MHz. It was concluded that such a loop antenna serves mainly to excite a dominant electrical dipole mode of operation for frequencies less than the lowest natural electrical resonance frequency of the helicopter itself, but greater than some frequency near the low end of the HF band. A limited set of measurements performed on a scale model of a helicopter generally supports the conclusions drawn from the numerical results predicted using NEC2. The reported result is of importance in so-called 'nap of the earth' HF communications from helicopters.*

1. INTRODUCTION

The method of moments [1] is used extensively in the design and analysis of wire antennas as well as the evaluation of the performance of such antennas on a variety of vehicles and structures [2]. The method has proved to be extremely useful for the evaluation of the performance of HF (3-30 MHz) antennas on aircraft, because of problems associated with measuring the overall performance either during flight tests or using scale models. For numerical analysis the aircraft fuselage and wings are modelled as wire-grid structures. The method is useful for examining the detailed performance of aircraft antennas in the HF band and as an engineering tool in designing such antennas.

Kubina [3] presents guidelines for numerically modelling wire grid structures. Along with other examples he also gives predicted and measured radiation patterns for a loop antenna on a CHSS-2/Sea King helicopter at frequencies of 2.6, 4.1, 6.0 and 8.1 MHz. The loop was mounted on the tailboom in the horizontal (x-y) plane. Owen [4] also gives guidelines for numerical modelling and presents measured and predicted radiation patterns for a helicopter mounted loop antenna at a frequency of 8 MHz. In this case the loop antenna was mounted in the vertical (x-z) plane below the tailboom of the helicopter. In [3] and [4] the emphasis appeared to be on the validation of computed results, and how best to achieve good comparisons with the measured results by 'tuning' the numerical model. Neither author examined the various radiation modes which could influence the radiation patterns. Burberry [5] points out that there are two modes of radiation present, that due to the antenna itself, as well as an additional mode due to the currents induced on the airframe by coupling with the antenna. From an examination of the results presented in [3] and [4] this author concluded that a longitudinal electrical dipole mode, corresponding with the

longest dimension of the helicopter fuselage, could at certain frequencies in the HF band be the dominant mode, depending on the mounting and orientation of the loop antenna.[1] A short study, restricted to the 2-15 MHz band which is used for HF communications over distances less than about 600 km, was therefore undertaken to test this hypothesis. It was not the purpose of the study to validate NEC2 for wire-grid models yet again. Consequently no attempt was made to 'tune' the numerical model.

2. DESCRIPTION OF THE NUMERICAL AND SCALE MODELS

In order to investigate the radiation patterns of a loop antenna on a helicopter, a wire grid structure, which can best be described as a generic model of a helicopter, was implemented for use in the Numerical Electromagnetics Code NEC2 [6]. The numerical model was based on top and side view scale model diagrams of an SA330B Puma helicopter available in a 1/32nd scale kit (no. PK-507) produced under the registered trademark 'Matchbox' by Lesney Products, London, England. The full scale dimensions of the helicopter are given in Table 1. Figure 1 shows line drawings of the wiregrid model and a sideview of the Puma helicopter. Also shown is a simple loop/dipole model suggested by Burke [7] for frequencies less than the fundamental electrical resonance frequency.

All wires used in numerically modelling the full scale helicopter fuselage were kept shorter than 1.5 m with a diameter of 0.2 m, except where noted. For the analysis the longer dimension of the helicopter was chosen to lie along the x-axis. The loop was modelled using three straight sections, each with a diameter of 0.03 m. The fourth side of the loop was formed by part of the tailboom, which was modelled as a rectangular grid structure. The overall dimension of the loop was 0.3 x 2.6 m and it was positioned on the starboard side below the tailboom. The longer loop dimension was parallel to the tailboom. The plane of the loop was at an angle of about 30 degrees to the x-z or $\phi = 0$ degrees plane, as defined by the rectangular or spherical coordinate system in the IEEE standard test procedures for antennas [8]. This offset in the plane of the loop was decided on after looking at possible means of attaching the loop to the airframe. The feedpoint was in the centre of the short loop section indicated in Figure 1(b). The shortest segment of length 0.06 m occurred in the feed region, giving a worst case segment length to diameter ratio of 2. Except for the number of main rotor blades this generic model in general resembles that of the Sea King used by Kubina in [3]. The total number of wires and segments used were 206 and 291 respectively. The numerical modelling guidelines of [3] and [4] were used.

Initially a single precision version of NEC2, restricted to a maximum of 300 wire segments, was used in order to speed up computer throughput. This version, however, predicted physically unacceptable negative radiation resistances at frequencies of 2 to 4 MHz as well as different null depths for conducting and perfectly conducting wire grids. Furthermore, scaling of the geometry of the full-scale numerical model at HF to dimensions appropriate for VHF model measurements by using the GS data card in NEC2, did not give the same

---

[1] *In a recent paper [11] Cox and Vongas draw attention to the fact that on a helicopter a loop antenna shunt feeds the fuselage/electric dipole, and that the helicopter/loop combination radiates in both loop and dipole modes for frequencies less than the lowest electrical resonance frequency of the helicopter.*

results as the unscaled version. The problems were referred to Burke who ascribed them to the use of electrically short segments at the source [7]. At this stage of the investigation, an improved operating system, which was reputed to use more accurate algorithms for evaluating functions, was installed on the computer used. Comparison of outputs run under the two different operating systems, showed that there were considerable differences (6 to 10 dB) in null depths and only marginal differences in peak values for various predicted radiation patterns. A double precision version of NEC2, which also resolved the problem of negative radiation resistances, was therefore implemented.

The numerical modelling was independently checked by a colleague on a VAX computer [9], but with smaller grid spacing and shorter wirelengths. This model used 880 elements. The predicted gain results at 5 MHz were, for practical purposes, identical to those obtained using the single precision version of NEC2 for the model considered in this paper. Two cases were considered in the independent study [9]. These were with a pair of the main rotor blades aligned with the fuselage and then rotated to make an angle of 45 degrees with the 'axis' of the fuselage. The differences in the predictions for these two cases were negligibly small at 5 MHz, suggesting that rotor modulation of the radiation pattern could be small at frequencies below the fundamental resonance frequency. Although this independent analysis indicated that the proposed numerical modelling was probably adequate for the purposes of this study, it was decided to validate the predicted results using a scale model.

A 1/22nd scale model of the helicopter, based on the kit data referred to above, was manufactured from wood. The wooden fuselage was covered with strips of thin brass shimstock. All overlapping joints were soldered to provide electrical continuity in any direction across the interface between strips. This does not necessarily model the expected surface conductivity of the helicopter particularly well because of the use of riveted panels and composite materials and the fact that the metal conductivities cannot always be scaled. No allowance was made in the model for doors or other apertures. The loop antenna on the model was fed via a coaxial cable connection on the inside of the model. The rear rotors as well as the horizontal rear stabiliser were made of metal. All provided good electrical contact with the fuselage. One of the problems which arose at this stage was whether to model the main rotors using carbon fibre composite or metal. Examination of a rotorblade of a Puma at a South African Air Force open day showed that the leading edge was protected by a metal strip which was electrically bonded to the rotor boss and the fuselage. It was concluded that it would be appropriate to treat the main rotors as conductors as had been done in the numerical modelling. This is essentially the same approach as used by Owen [4].

The numerical modelling frequencies for the 22:1 scale model of the helicopter ranged from 44 to 330 MHz in 22 MHz steps. As a check on the accuracy of the computations, gain calculations were made at 5 degree increments in azimuth and elevation and the average gain computed. For perfectly conducting wires the average gain in free space should be 1.0 [6]. The number of segments of the wires in the feed region and other wires connected to these were varied in order to obtain the best overall average gain over the frequency range. The position of the feed segment was also changed to ensure the best overall average gain.

The lowest segment length to diameter ratio of about 2 was in the feed region. The extended thin-wire kernel option of NEC2 was tried but gave no real improvement in the average gain predicted over the frequency range. In general the guidelines for numerical modelling given by [3] and [4] were followed. The segment lengths of all wires connected to the shorter loop sections were made approximately the same length as the segments used in the loop sections. The diameters of these wires were made 0.08 m in order to limit the change in diameter between connected wires to a factor of about 2.5. In this case this was found to give satisfactory results.

Figure 2 shows the predicted average gains, normalisation gain factors and directivities, corrected for the deviation in the average gain from the expected value of 1.0, for the numerical model of the 22:1 helicopter scale model using perfect and brass conductors. The range of modelling frequencies from 44 to 330 MHz corresponds to a full scale frequency range of 2 to 15 MHz. Application of the average gain correction for the brass wire model gives a corrected directivity which agrees to within 0.01 dB with that shown for a perfect conductor in Figure 2(a). Below 200 MHz the directivity is approximately that expected for a dipole. It was concluded that the numerical model would be adequate to test the hypothesis that the dominant radiation mode for frequencies less than the fundamental resonance frequency, is the longitudinal dipole mode.

A limited set of radiation pattern measurements was made on the 22:1 scale model at frequencies of 110 and 220 MHz, corresponding to full-scale frequencies of 5 and 10 MHz respectively. All measurements were performed at the National Antenna Test Facility at Paardefontein, north of Pretoria, South Africa [10]. The choice of frequencies was largely dictated by the level of interference in the FM and TV broadcast bands at the site. The source antenna was a horizontally polarised ground arrayed log-periodic array. A 10 dB attenuator was inserted at the feedpoint of the loop antenna in order to provide a nearly constant load for the receiver. This restricted the overall sensitivity of the system and may have influenced the measured results. The orientation of the model was adjusted depending on the cut and required field component relative to the model's coordinate system.

3. COMPARISON BETWEEN PREDICTED AND MEASURED RESULTS

The maximum path length on the helicopter which could support an electrical dipole-like resonance was estimated to be about 19.2 m. This is measured along the length of a rotor blade, down the drive shaft, back along the tailboom and out to the end of the rear control surface. For an electrical dipole this corresponds to a fundamental resonance frequency of 7.8 MHz, corresponding to a scaled frequency of 172 MHz. For the helicopter this frequency may be reduced because of the diameter to length ratio of the fuselage itself compared with a thin dipole, and possible capacitive loading effects of the main and tail rotors. The selected measurement frequencies of 110 and 220 MHz straddle the fundamental resonance frequency of the model.

Because of the difference in the implementations of the feedpoints in the numerical and physical scale models, it is expected that a comparison of the predicted and measured input impedances for the loop antenna will at best be of a qualitative nature. The feed for the

numerical model was in the centre of the short segment marked as 'feedpoint' in Figure 1(b). In the case of the scaled physical model this loop segment was fed at the junction point at the fuselage. Figure 3 compares the predicted and measured input impedances for the physical scale model. Only half of the Smith chart is shown. The measured results indicate that the real part of the input impedance increases from 1 Ohm to about 60 Ohms over a range of 44 to 242 MHz. Over the same range the inductive part increases from about 4 to 340 Ohms. Figure 4 compares the measured input impedances for the loop antenna with and without the main and tail rotors. The effect of removing the rotors is relatively small, suggesting that rotating rotors will not modulate the loop's input impedance by much. One can see what appears to be a relatively small effect in the measured input impedance for the model due to the fundamental resonance frequency at 176 MHz. In the case of the fuselage with no rotors, the probable effect of a slightly higher fundamental resonance frequency of 220 to 242 MHz can be seen. The length of the full scale fuselage excluding rotors is about 13.8 metres, corresponding to a scaled (model) halfwave resonance frequency of 239 MHz.

Ideally an examination of the relative amplitudes of the theta- and phi- components of the electric field in the x-y plane will show the difference in the relative importance of the loop and electrical dipole fields, $E(\theta)$ and $E(\phi)$ respectively in this case. In retrospect it would have been advisable to mount the loop antenna symmetrically with respect to the tailboom and below it in the x-z plane, instead of at an angle of 30 degrees, in order to enhance the differences in the fields.

For all helicopter radiation patterns shown in the figures one pair of rotors was aligned with the length of the fuselage. Also shown in Figures 5, 6, 8 and 9 are the expected normalised radiation patterns for a dipole placed along the 'axis' of the fuselage. Because of time limitations on the use of the test range no measurements were made in the vertical y-z plane orthogonal to the fuselage 'axis'. The alignment of the rotors in the helicopter schematic in the figures are for illustrative purposes only. The use of symbols to indicate orientation are as follows: F = forward, S = starboard, P = port, T = top, B = bottom and A = aft.

Figures 5 and 6 show normalised comparisons of measured and predicted radiation patterns for a model frequency of 110 MHz, corresponding to a full-scale frequency of 5 MHz, for x-y and x-z planes respectively. In Figure 5 the model's measured and predicted results in the horizontal x-y plane at 110 MHz (5 MHz full-scale) for the $E(\theta)$ and $E(\phi)$ fields are in reasonable agreement. Except for the depth of the nulls, the $E(\phi)$ fields resemble the dipole radiation pattern. The $E(\theta)$ fields can be attributed mainly to the loop antenna with null filling at broadside being caused by vertical currents on the fuselage. Figure 6 shows the model's measured and predicted radiation patterns at 110 MHz for the $E(\theta)$ and $E(\phi)$ fields in the vertical x-z plane. In this case the $E(\theta)$ field can reasonably be expected to be a combination of the loop and dipole modes. The predicted and measured $E(\theta)$ patterns are again in reasonable agreement. However, they tend to resemble only the pattern of an electrical dipole aligned with the fuselage 'axis', with little contribution evident for the loop antenna. Comparison of the measured and predicted $E(\phi)$ fields is however poor. Some of the differences for this field component are probably due to the differences in the feed arrangements for the numerical and physical models referred to earlier. The lack of

measuring sensitivity and stray fields due to scattering from coaxial cables may also have influenced the measurement of the $E(\phi)$ component. The predicted $E(\phi)$ field resembles that of a small loop antenna in the x-y plane. This may be a residual effect of the offset loop antenna which is mainly in a vertical plane.

A residual electrical dipole field, believed to be attributable to the feed arrangement for the numerical model, can be seen in the $E(\theta)$ field illustrated in Figure 7 which shows the predicted fields in the y-z plane. The nulls are approximately aligned with the axis of the short feed section. The $E(\phi)$ component is nearly omni-directional, with a variation of less than 1 dB, as would be expected for a predominantly electrical dipole-like field.

Figures 8 and 9 compare the predicted and measured $E(\theta)$ and $E(\phi)$ fields for the model at 220 MHz (10 Mhz full scale) for the x-y and x-z planes respectively. It should be noted that the rotor blades on the full scale helicopter have a diameter of 15 m, corresponding to a resonant halfwave dipole of 10 MHz. In the case of the x-y plane, shown in Figure 8, the agreement is relatively good for the $E(\theta)$ component. The measured $E(\phi)$ component once more tends to resemble the dipole field, but compares relatively poorly with the predicted field. Figure 9 illustrates the case for the x-z plane. Except for the depth of the null the agreement between the measured and predicted $E(\theta)$ fields is reasonable. It is believed that the main rotor blade resonance influenced the predicted depth and position of the null. The effect of changing the frequency to 215 MHz is also shown for comparison. The $E(\phi)$ components resemble each other superficially. Differences are ascribed to problems encountered during the measurements due to low sensitivity and scattering from coaxial cables. The position and depth of null of the predicted $E(\phi)$ component in the x-y plane as shown in Figure 8 was found to be not nearly as sensitive to changes in frequency compared to the $E(\theta)$ field shown in Figure 9.

The results illustrated in Figures 5 and 6 were typical of predictions up to about 176 MHz which was near the fundamental electrical resonance frequency of the model helicopter. However, it was found that as the frequency for the scale model was decreased to 44 MHz (2 MHz full scale), the predicted contribution of the loop antenna to the overall radiation pattern increased steadily until the loop's contribution to the radiated field compared with that of the dipole, as shown in Figure 10. Also shown are the fields computed for the simple electrical dipole/loop antenna combination of Figure 1(c) as suggested by Burke [7]. The dimensions of the electrical dipole/loop combination are similar to the overall helicopter and loop antenna combination. The wire diameters were 0.02m. The null-filling evident in the predicted radiation pattern for the dipole mode for the helicopter model is ascribed to the asymmetric placement of the loop antenna, with resultant circumferential currents on the fuselage in the x-y plane. Above 44 MHz for both the helicopter and simple case, the radiated field due to the electrical dipole mode exceeded that due to the loop. In both cases at 110 MHz (5 MHz full scale) the radiated field due to the electrical dipole mode was predicted to be about 15 dB greater than that due to the loop. At 220 MHz (10 MHz full scale) for the simple model, the electric field due to the loop is predicted to be more than 25 dB less than that due to the electrical dipole.

Examination of the predicted radiation patterns for the model helicopter between the

fundamental resonance frequency of about 176 and 330 MHz (8 MHz and 15 MHz full scale), shows that the electrical dipole field component becomes more distorted. Examples of this effect are shown in Figures 11 to 13 for the principal planes for the model at 330 MHz (15 MHz full scale). Figure 12 shows a similar residual electrical dipole effect, possibly due to the feed segment and also observed in Figure 7. It is believed that the distortion of the electrical dipole field is due to the increasing relative importance of various higher order current modes discussed in [5] as the frequency is increased. It is, however, clear that there is still a substantial contribution from the electrical dipole mode of radiation for the helicopter.

4. DISCUSSION

On the basis of reasonable agreement between measured and predicted results for the largest electrical field components, it is concluded that the dominant radiation mode for a helicopter-borne loop antenna lying in a plane containing the longest dimension of the fuselage, tends to be electrical dipole-like at frequencies below the fundamental resonance frequency but above some frequency at the low end of the HF band. For the full scale example considered here this low end frequency is of the order of 2 MHz. A strong electrical dipole-like component persists up to 15 MHz for the example considered. However, as frequencies increase above the fundamental electrical resonance, the effect of higher order current modes on the fuselage and main rotors on the radiation pattern become increasingly important. The resultant pattern is thus a composite of the electrical dipole-like field, fields due to the higher order current modes and any residual effect due to the loop antenna itself.

'Nap of the earth' (NOE) HF communications is restricted to the lower half of the HF band by ionospheric propagation and require high take-off angles. Most helicopters and aircraft will have fundamental electrical resonances at frequencies in the HF band because of their physical size. For this reason it is important that aircraft antenna engineers concerned with NOE systems consider the entire helicopter as the radiating structure. It is suggested that it could be worthwhile examining ways in which the dipole mode could be directly stimulated in order to improve efficiency and matching.

5. ACKNOWLEDGEMENTS

The author gratefully acknowledges the assistance of the following: Dr. D. E. Baker of EMLab for accommodating the measurements described above in a busy measuring schedule of his own, Mr. B. J. van der Riet of the Division for Microelectronics and Communications Technology, Council for Scientific and Industrial Research for help at the antenna test range, Mr. F. J. van der Walt for the preparation of the polar diagrams and Mr. J. M. Brand for the construction of the helicopter scale model.

6. REFERENCES

[1] Harrington, R. F.: "Field Computation by Moment Methods". Robert E. Krieger Publishing, Malabor, Florida, 1982

[2] Miller, E. K.: "Numerical Modelling Techniques for Antennas". The Performance of Antennas in Their Operational Environment, AGARD Lecture Series No. 131, NATO, Neuilly Sur Seine, France, pp. 7-1 to 7-29, 1983.

[3] Kubina, S. J.: "Numerical Modelling Methods for Predicting Antenna Performance on Aircraft", ibid., pp. 9-1 to 9-38.

[4] Owen, J. I. R.: "Wire Grid Modelling of Helicopter HF Antennas", IEEE International Antennas and Propagation Symposium Digest, pp. 722 to 725, 1980.

[5] Burberry, R. A.: "HF Loop Antennas for Air, Land and Sea Mobiles", IEE Second Conference on HF Communication Systems and Techniques, London, pp. 18 to 22, 1982.

[6] Burke, G. J. and Poggio, A. J.: "Numerical Electromagnetic Code (NEC) - Method of Moments". Technical Document NOSC 116, Naval Electronic Systems Command (ELEX 3041), Naval Ocean Systems Center, San Diego, California, 92152.

[7] Burke, G. J.: Lawrence Livermore Laboratory, Livermore, California - Private communication.

[8] IEEE Standard Test Procedures for Antennas, IEEE Std. 149-1979 (IEEE Press, New York, 1979)

[9] Cloete, J. H.: Department of Electronic and Electrical Engineering, University of Stellenbosch, Stellenbosch, South Africa - Private communication.

[10] Baker, D. E.: "Development and Evaluation of the 500 M Ground-reflection Antenna Test Range of the CSIR, Pretoria, South Africa", Proceedings of the Annual Conference of the Antenna Measurement Techniques Association, San Diego, California, 2-4 October 1984, pp. 5A4-1 to 5A4-16.

[11] Cox, J. W. R. and Vongas, G.: "Calculated and Measured Radiation Characteristics of an HF Loop Antenna Mounted on a Helicopter", Fifth International Conference of HF Radio Systems and Techniques, IEE Conference Publication No. 339, July 1991.

Table 1. Dimensions of the Puma SA330 helicopter used in the numerical and scale models.

(1)	diameter of main rotor (4 blades)	15 m
(2)	overall length (rotors turning)	18.15 m
(3)	height	5.14 m
(4)	fuselage length including rear rotors (scaled from kit data)	14.82 m

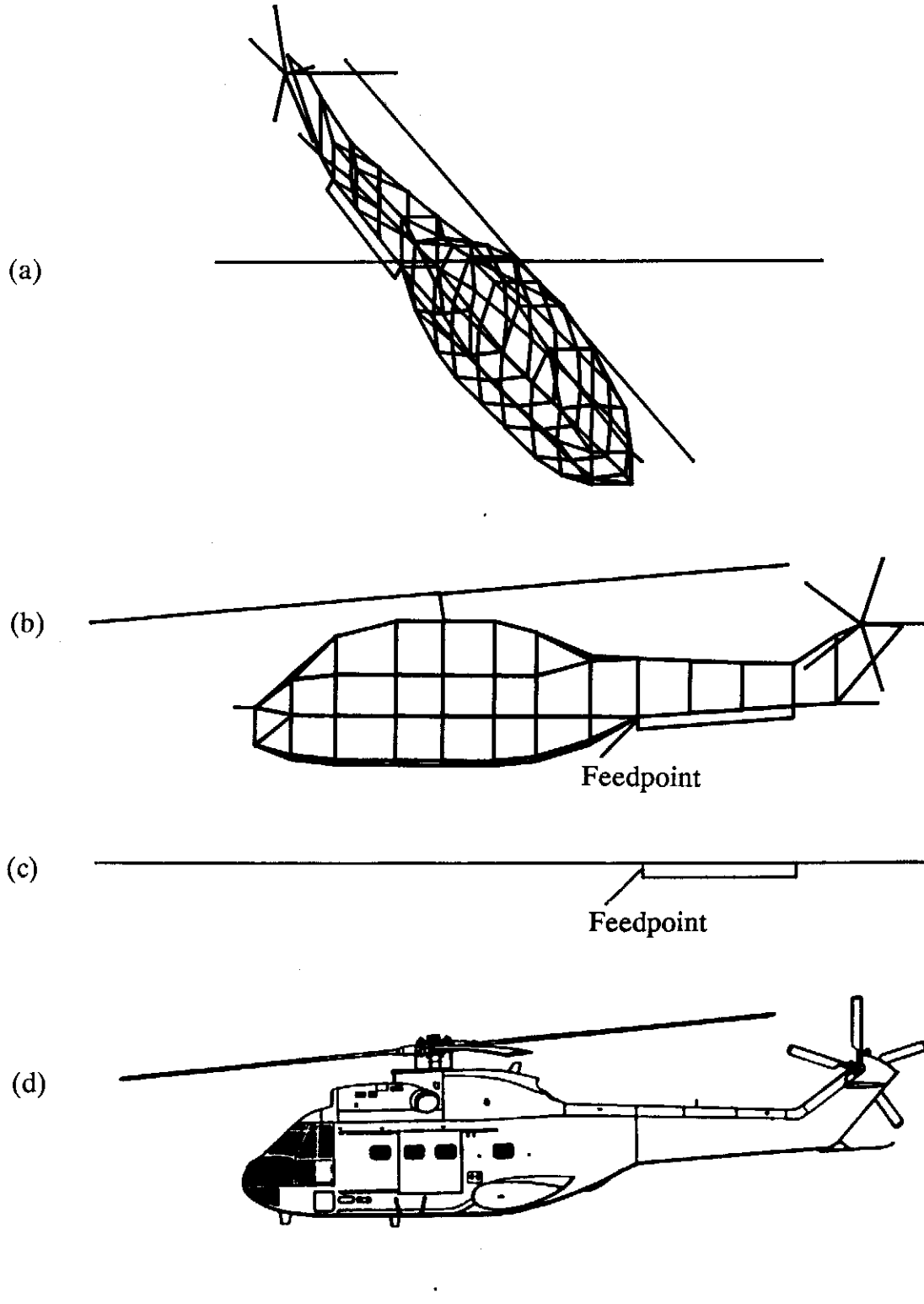

Figure 1. Figures (a) and (b), isometric and side views of the wiregrid model of a SA330 PUMA helicopter; (c), simple low HF loop/dipole model; (d) line drawing of the helicopter.

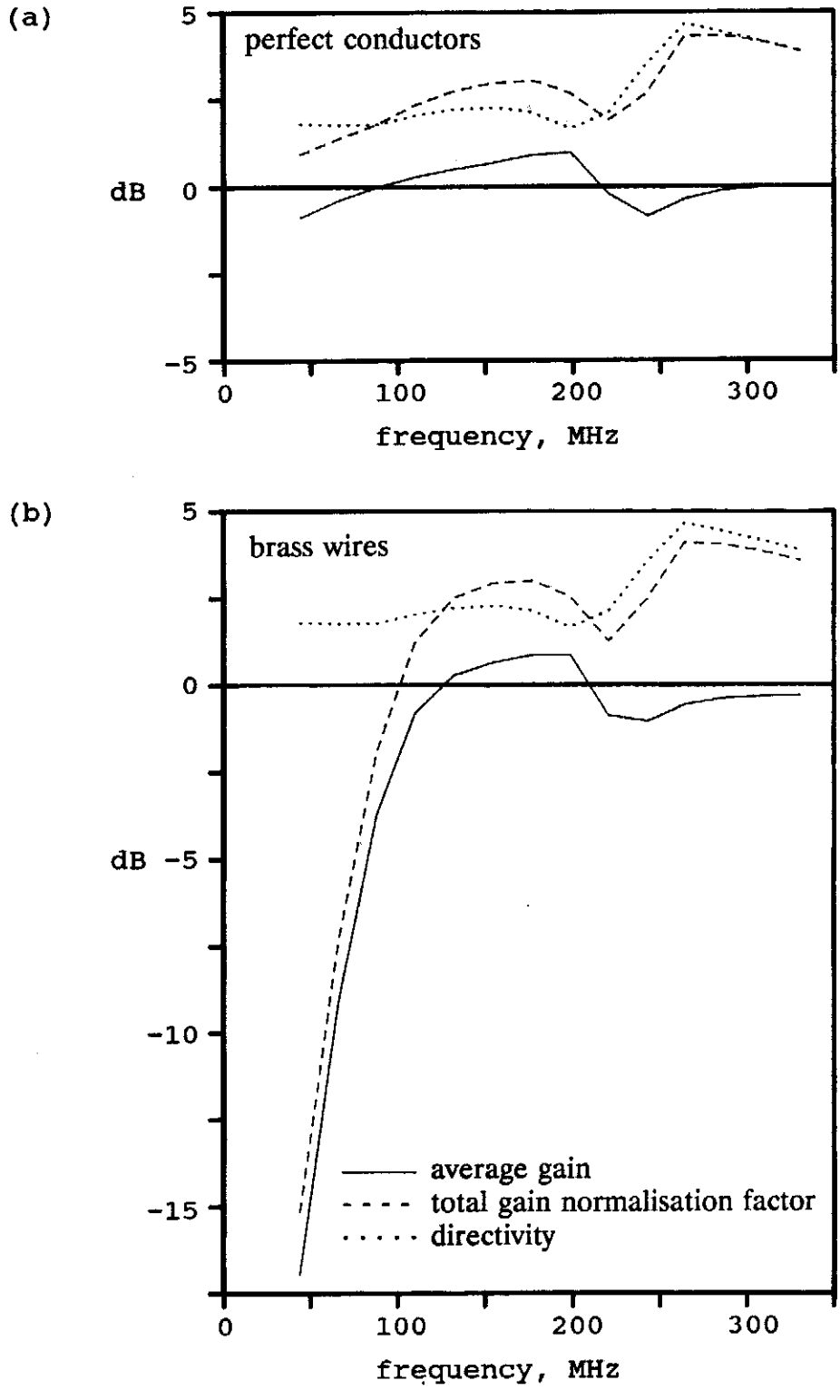

Figure 2. Average gains, predicted total gain normalisation factors and corrected directivities for the helicopter model with (a) perfectly conducting and (b) brass wires.

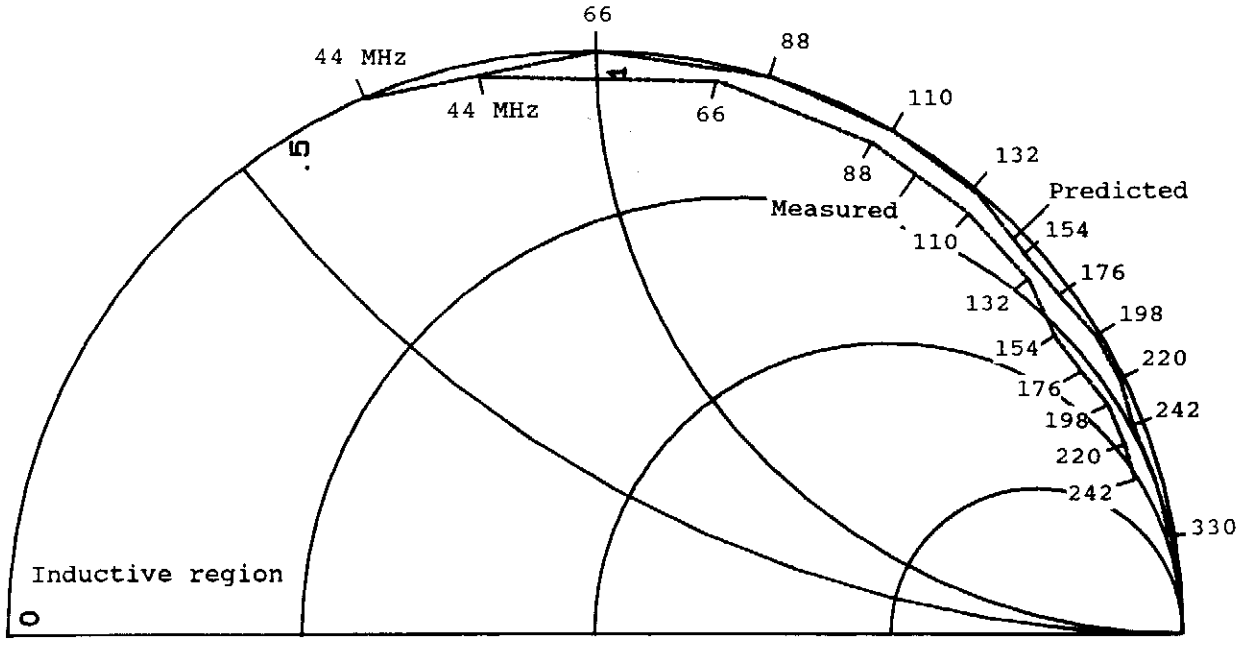

Figure 3. Comparison of predicted and measured antenna input impedances for the complete helicopter scale model. Only the upper half of the Smith chart is shown. (Normalisation - 50 ohms)

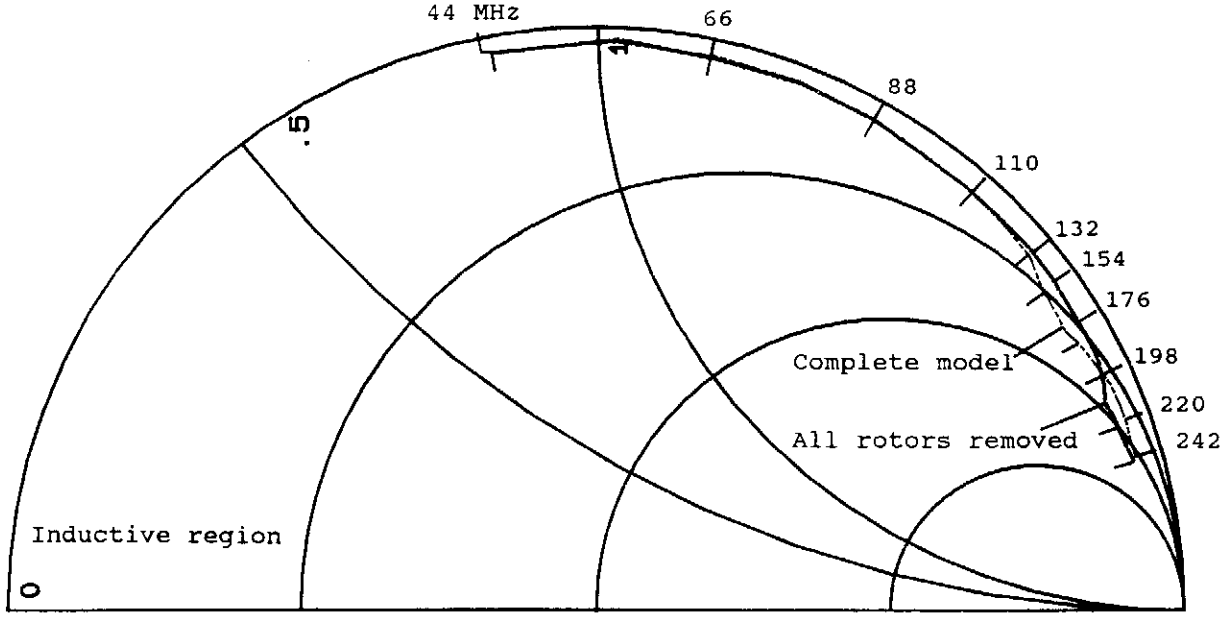

Figure 4. Comparison of measured antenna input impedances for the complete helicopter scale model and the fuselage after removal of all rotors. Only the upper half of the Smith chart is shown. (Normalisation - 50 ohms)

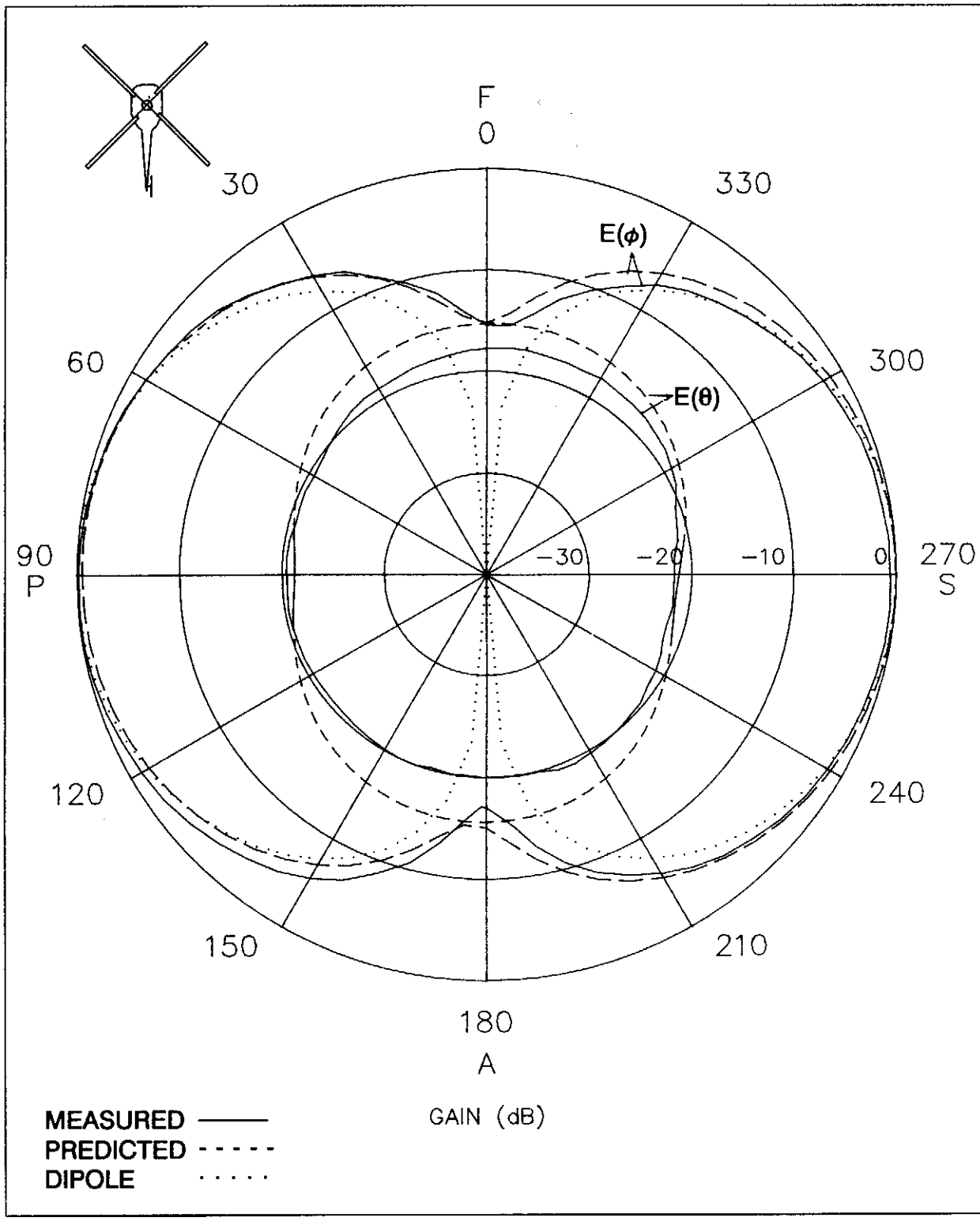

Figure 5. Comparison of normalised measured and predicted radiation patterns at 110 MHz in the x-y plane. Predicted patterns normalised to $E(\phi)$ = 1.1 dB. Normalised dipole pattern shown for reference.

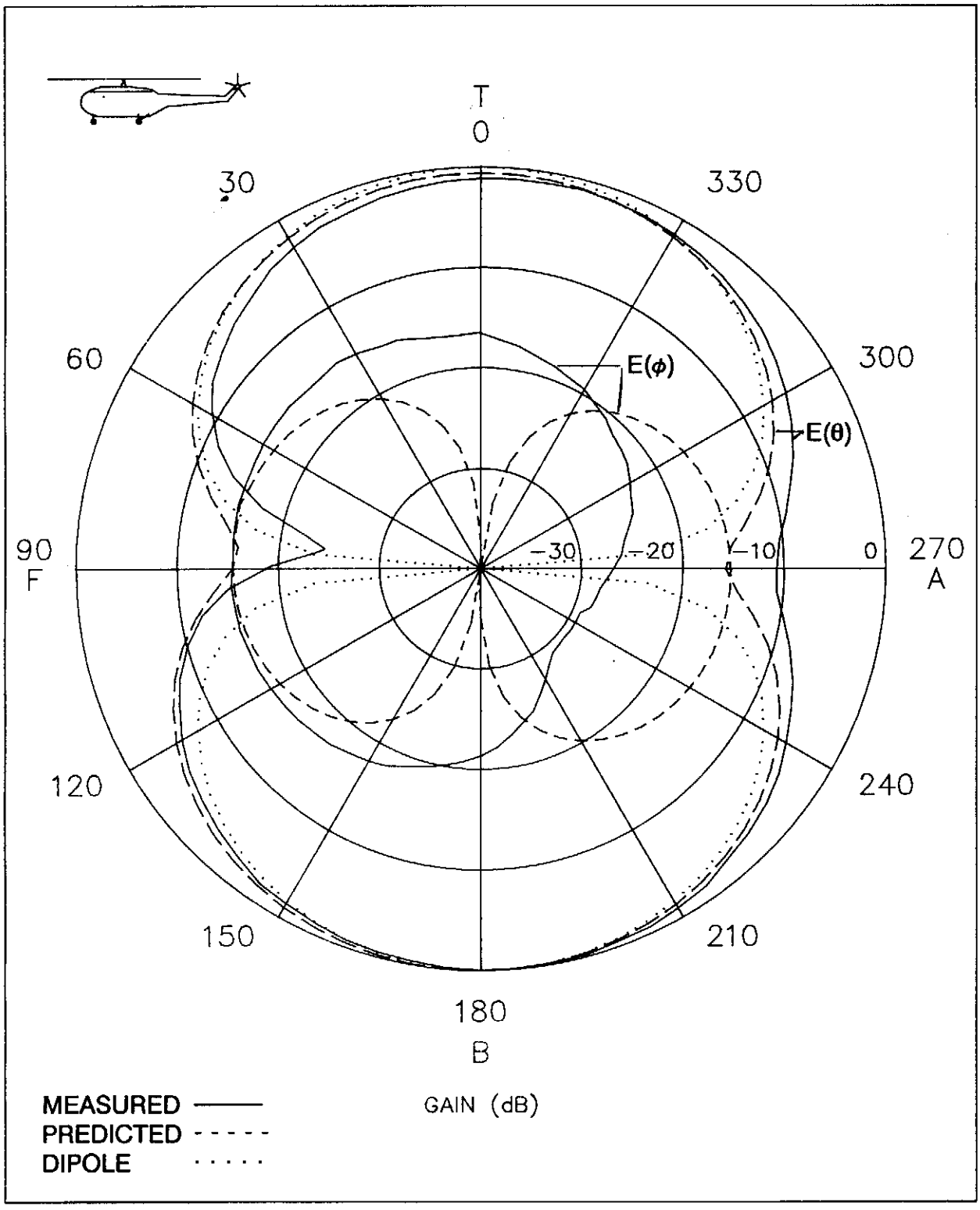

Figure 6. Comparison of normalised measured and predicted radiation patterns at 110 MHz in the x-z plane. Predicted patterns normalised to E(θ) = 1.3 dB. Normalised dipole pattern shown for reference.

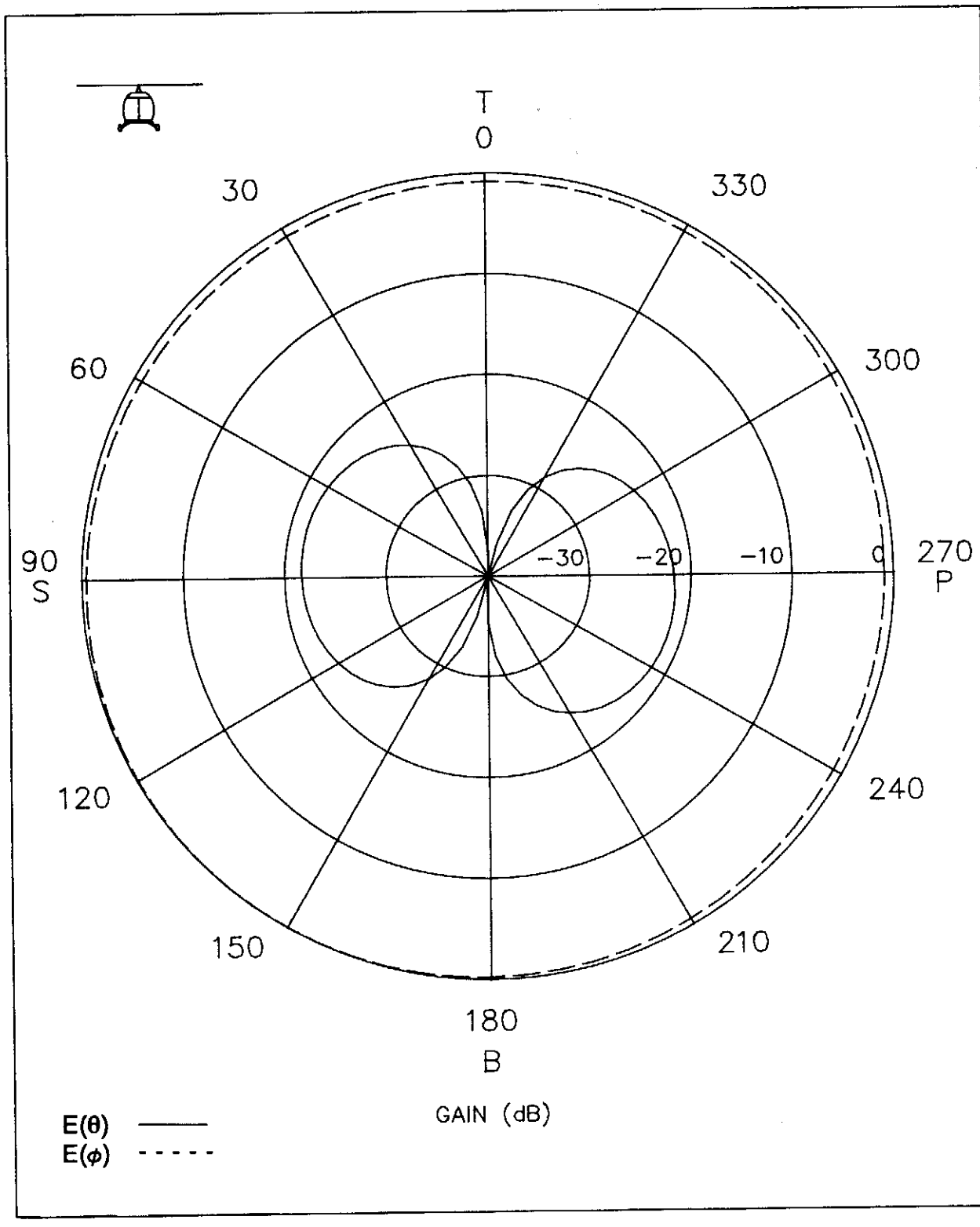

Figure 7. Predicted fields for the helicopter model in the y-z plane at 110 MHz. Patterns normalised to $E(\phi)$ = 1.5 dB.

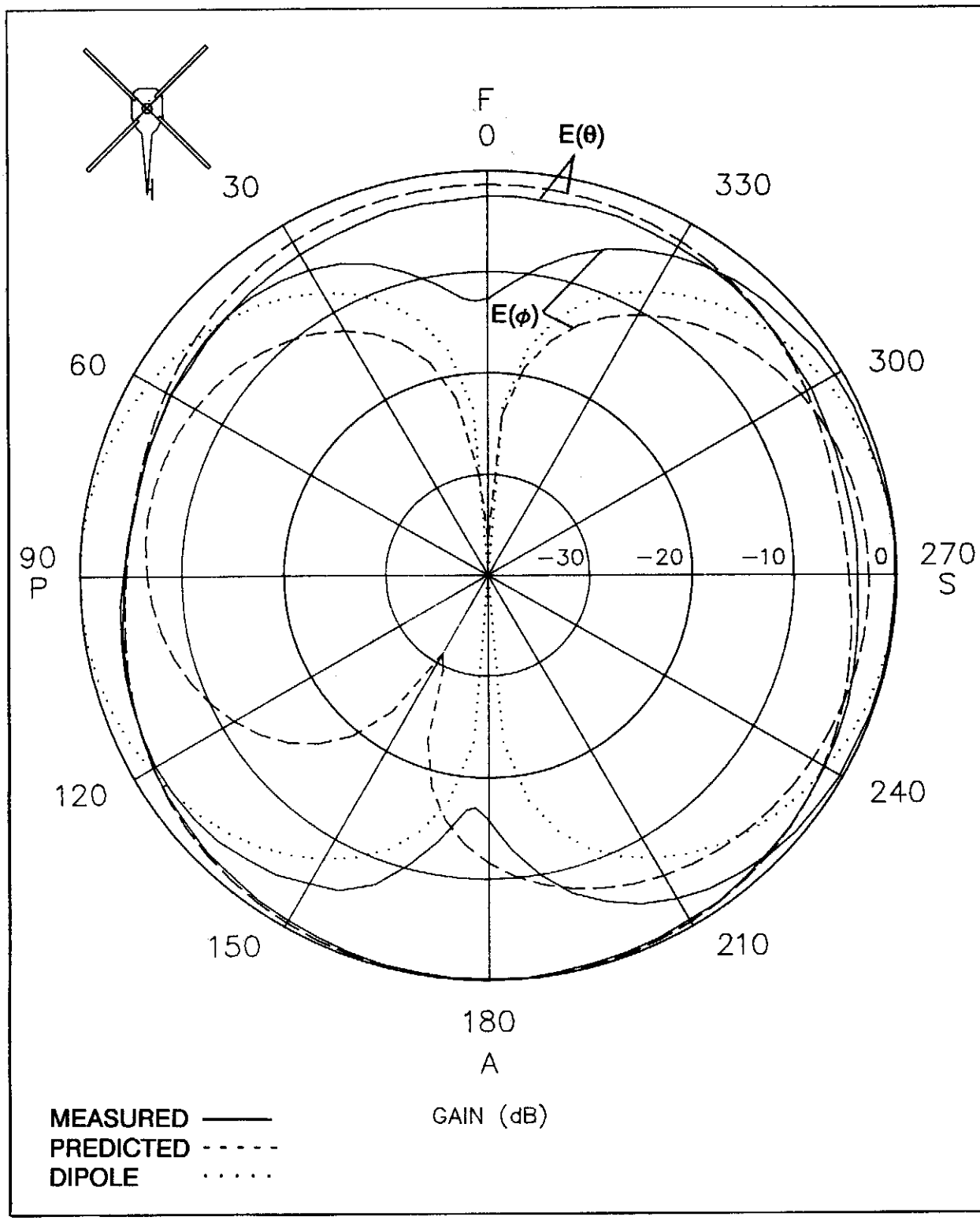

Figure 8. Comparison of normalised measured and predicted radiation patterns at 220 MHz in the x-y plane. Predicted patterns normalised to E(θ) = 0.6 dB. Normalised dipole pattern shown for reference.

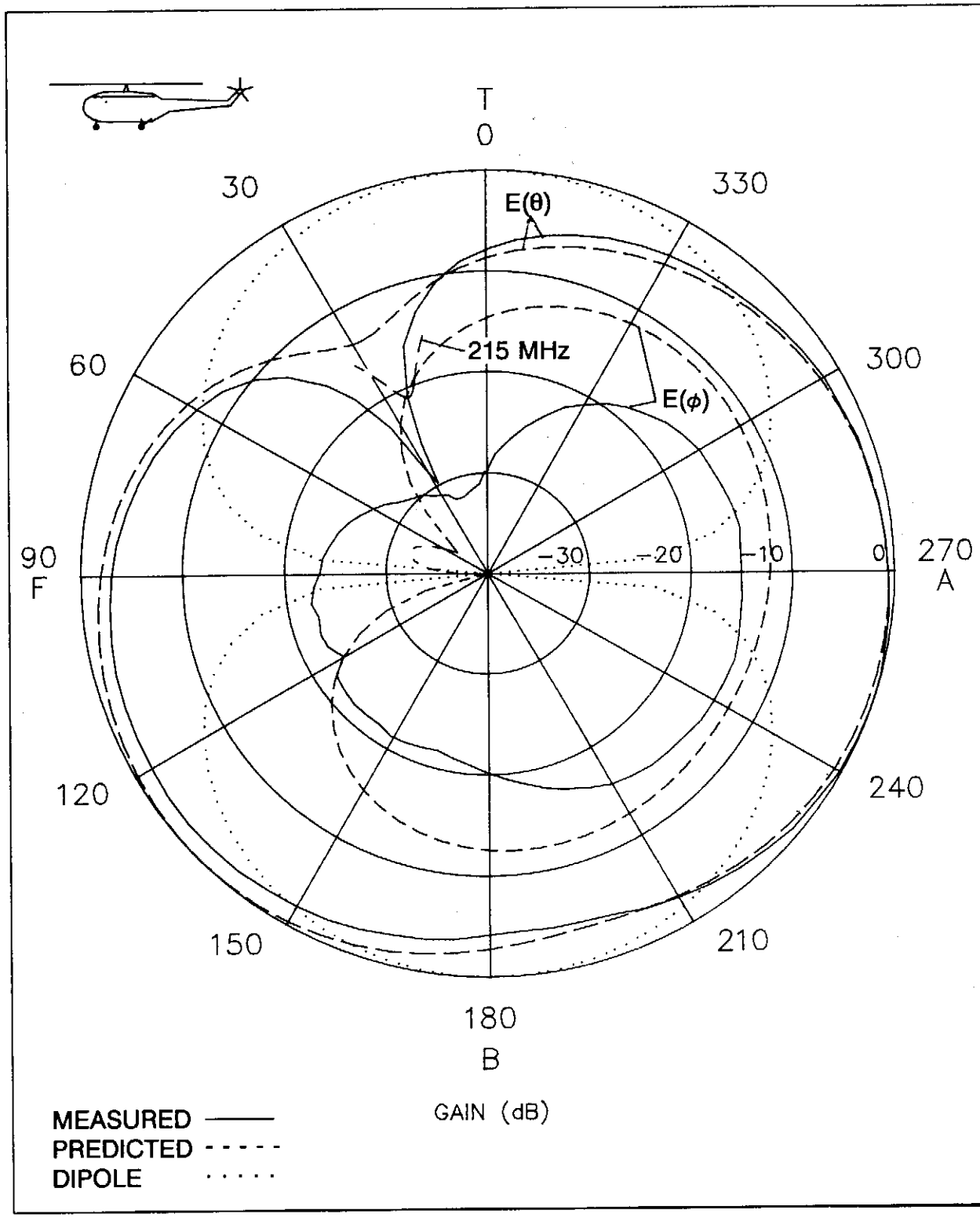

Figure 9. Comparison of normalised measured and predicted radiation patterns at 220 MHz in the **x-z** plane. Predicted patterns normalised to $E(\theta)$ = 1.1 dB. Normalised dipole pattern shown for reference.

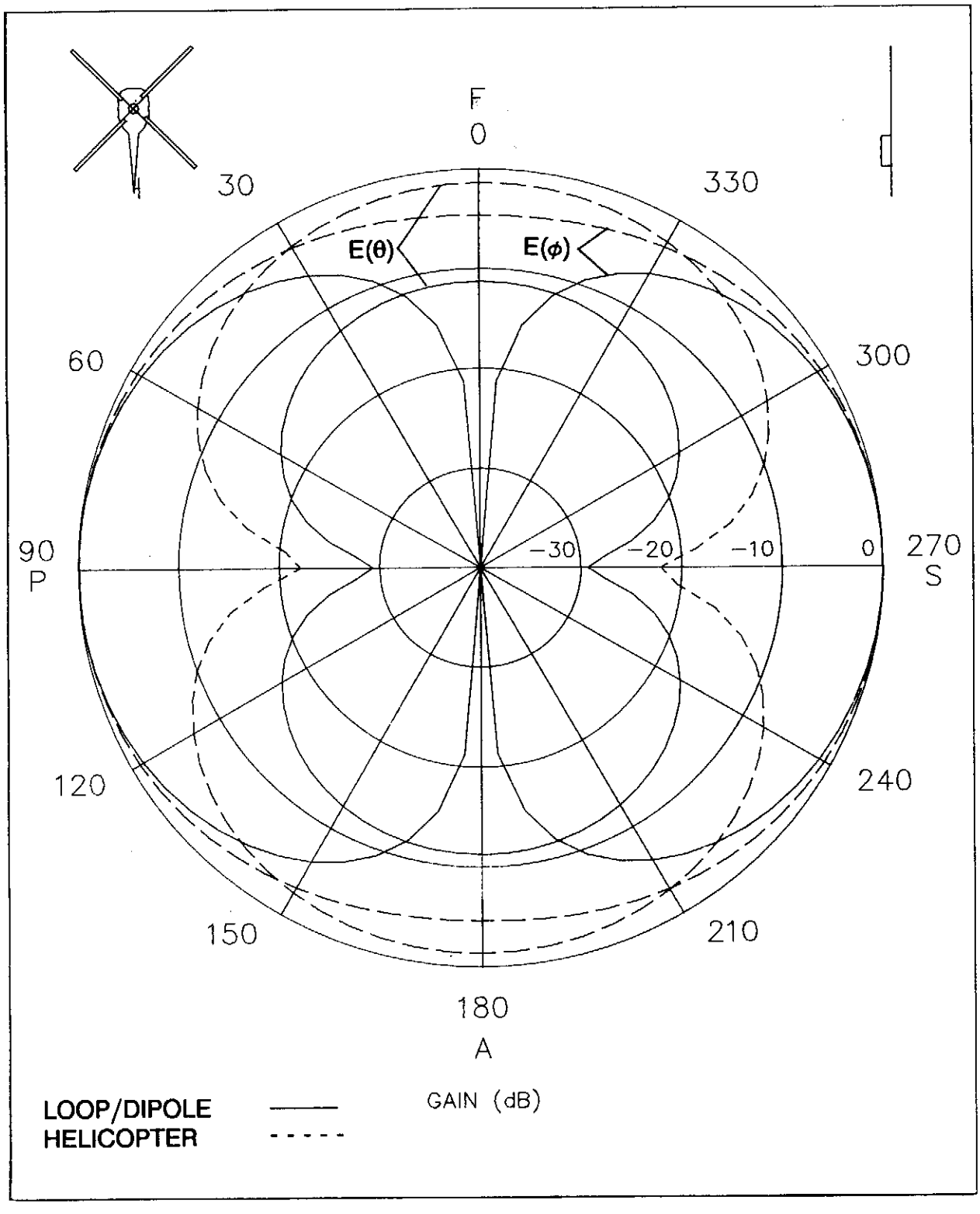

Figure 10. Comparison of predicted radiation patterns at 44 MHz for the scaled helicopter borne loop antenna and the simple loop/dipole model, using brass conductors for both cases. Helicopter patterns normalised to $E(\phi)$ = -16.5 dB. Loop/dipole patterns normalised to $E(\phi)$ = -18.0 dB. The loop is in the x-z plane. Patterns are for the x-y plane.

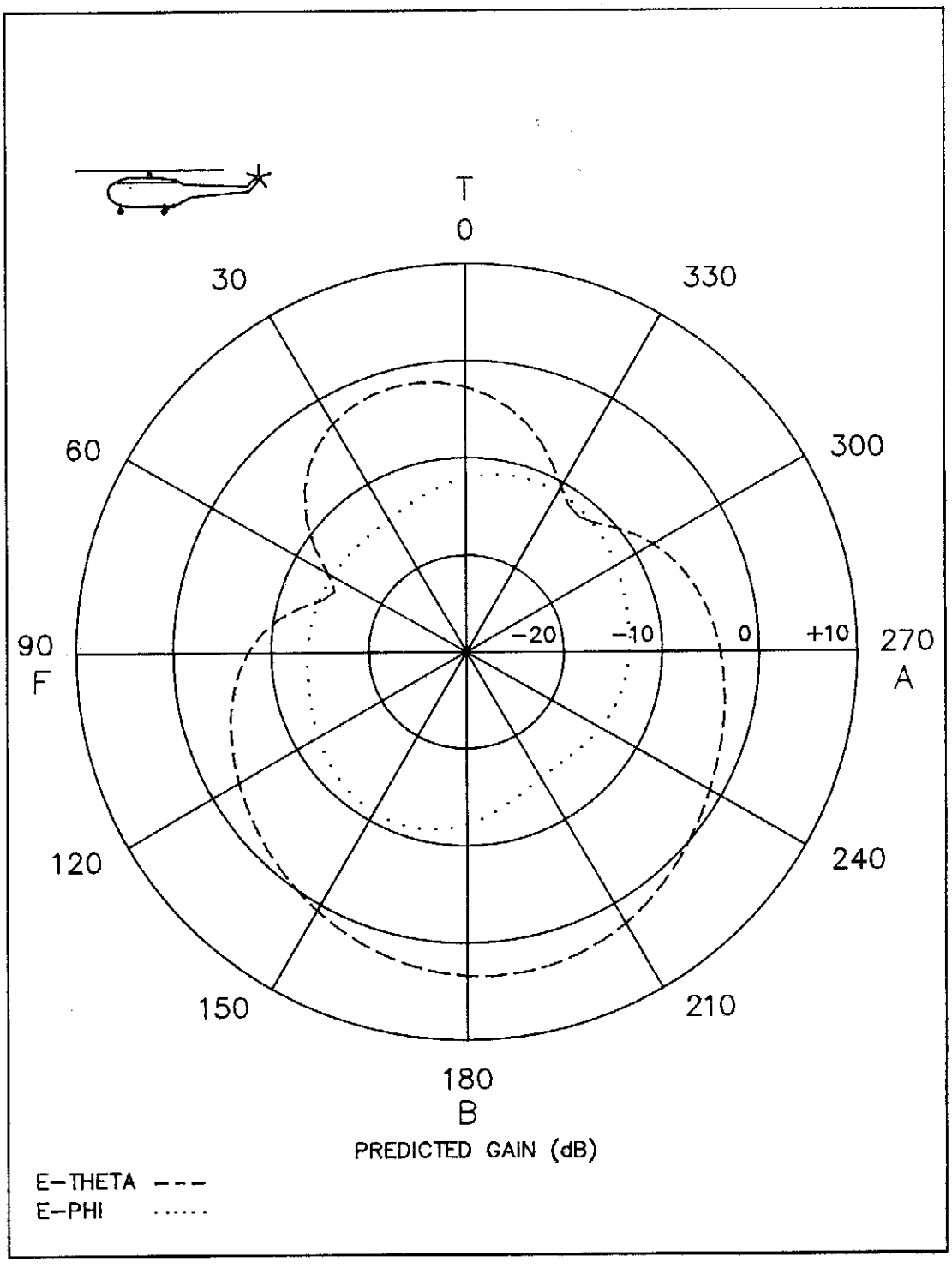

Figure 11. Predicted gains for the helicopter model in the x-z plane at 330 MHz. Brass conductors.

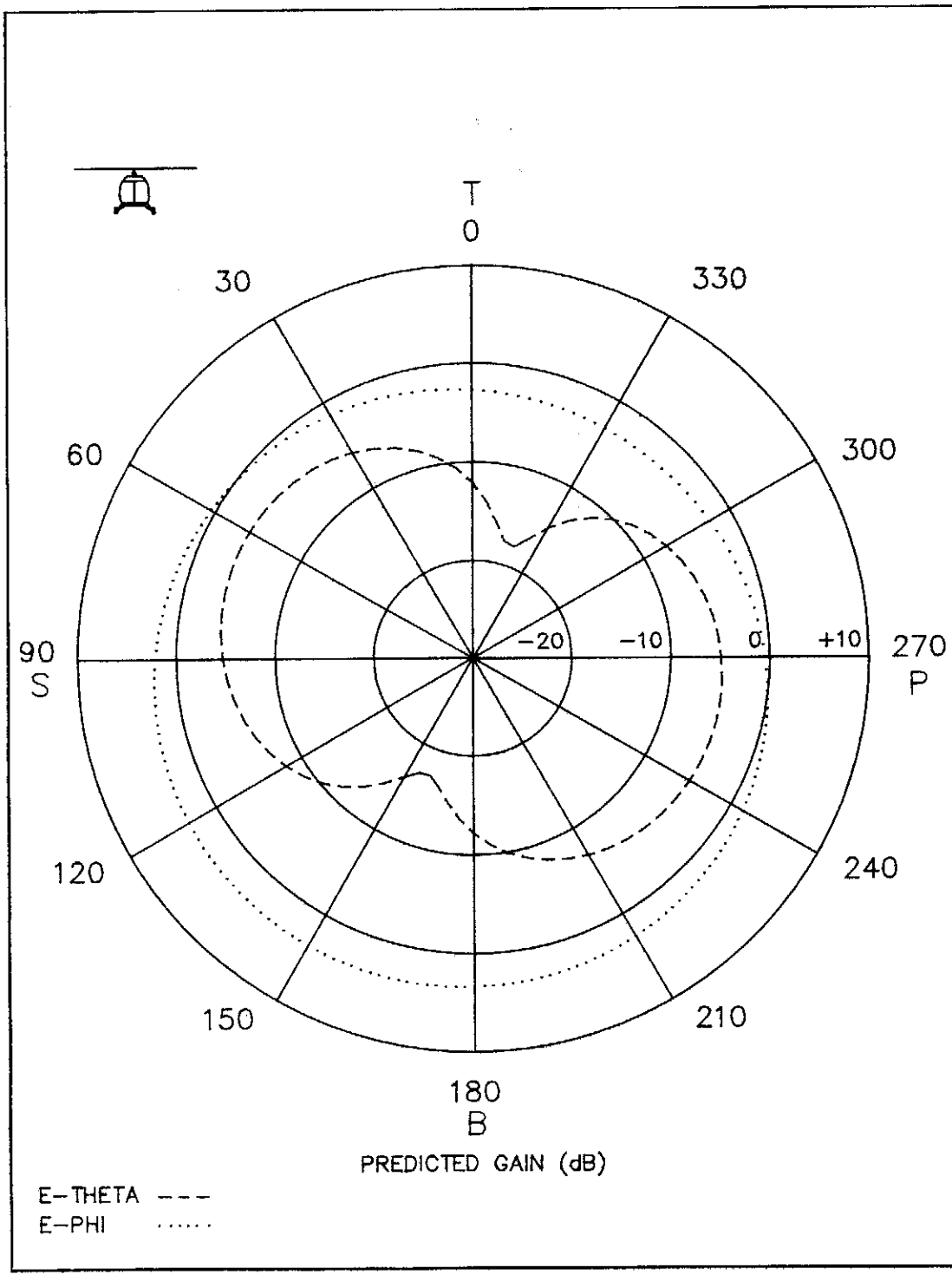

Figure 12. Predicted gains for the helicopter model in the y-z plane at 330 MHz. Brass conductors.

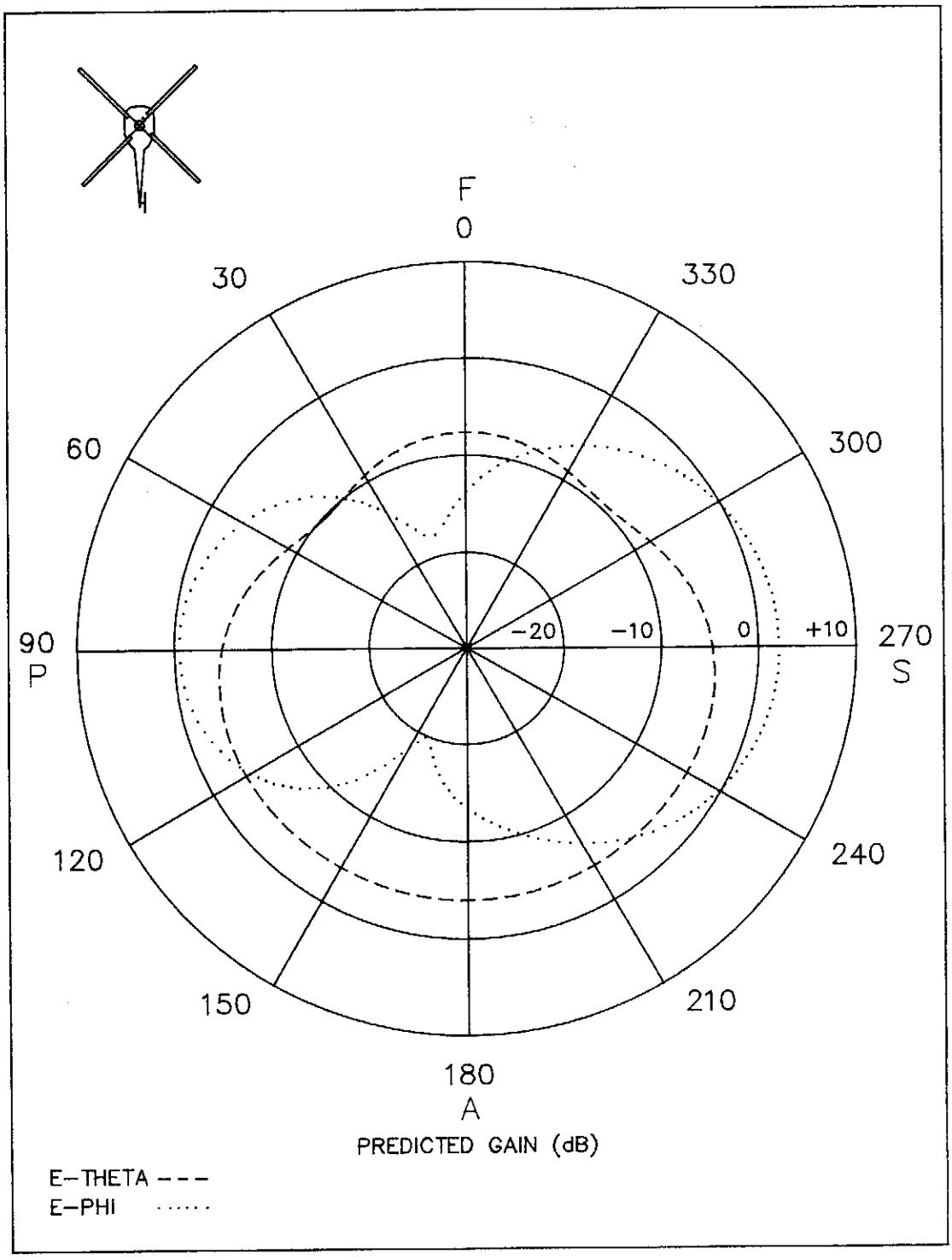

Figure 13. Predicted gains for the helicopter model in the x-y plane at 330 MHz. Brass conductors.